

Palladium Catalyzed Ethylene/Methyl Acrylate Copolymerization: Moving from the Acenaphthene to the Phenanthrene Skeleton of Alfa-Diimine Ligands

*Anna Dall'Anese,[†] Vera Rosar,^{†,§} Luca Cusin,^{†,§} Tiziano Montini,^{†,¥} Gabriele Balducci,[†] Ilaria
D'Auria,[‡] Claudio Pellecchia,[‡] Paolo Fornasiero,^{†,¥} Fulvia Felluga,[†] Barbara Milani*[†]*

[†] Dipartimento di Scienze Chimiche e Farmaceutiche, Università di Trieste, Via Licio Giorgieri
1, 34127 Trieste, Italy

[¥] INSTM Trieste Research Unit and ICCOM-CNR Third Parties Research Unit, University of
Trieste, Via Licio Giorgieri 1, 34127 Trieste, Italy

[‡]Dipartimento di Chimica e Biologia "A. Zambelli", Università di Salerno, via Giovanni Paolo II
132, I-84084 Fisciano (SA), Italy.

KEYWORDS. Palladium, Polar vinyl monomers, copolymerization, functionalized polyolefins,
nitrogen-donor ligands, alfa-diimines, ethylene

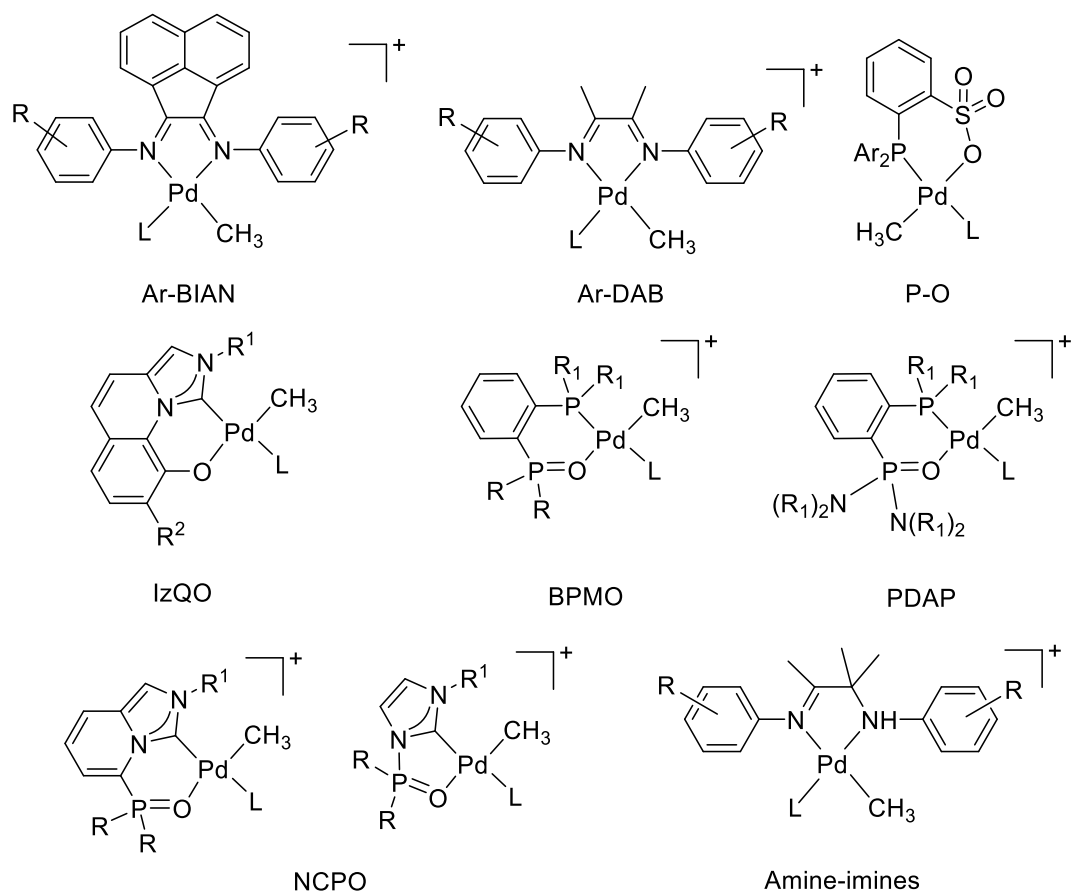
ABSTRACT. The development of efficient homogeneous catalysts for the synthesis of functionalized polyolefins is a challenging topic. Palladium(II) complexes with α -diimine ligands having a phenanthrene skeleton and 2,6-disubstituted aryl rings (Ar-BIP) were synthesized, characterized and tested as precatalysts in the copolymerization of ethylene with methyl acrylate. The direct comparison with analogous complexes having the corresponding α -diimines with an acenaphthene skeleton (Ar-BIAN) was performed. X-ray characterization in solid state and NMR analysis in solution of both neutral, $[\text{Pd}(\text{Ar-BIP})(\text{CH}_3)\text{Cl}]$, and monocationic $[\text{Pd}(\text{Ar-BIP})(\text{CH}_3)(\text{NCCH}_3)][\text{PF}_6]$ complexes, indicate that the Ar-BIP ligands have a higher Lewis basicity and are more strongly coordinated to the metal center than the Ar-BIAN counterparts. Therefore, the Pd-(Ar-BIP) cationic complexes can be regarded as electron-rich metal cations. In addition, they create a higher steric congestion around palladium than Ar-BIAN, regardless of the substituents on the aryl rings. The monocationic species generate active catalysts for the ethylene/methyl acrylate copolymerization leading to copolymers with M_n values up to 37000 and a content of polar monomer of 5.3 mol %. The detailed study of the catalytic behavior points out that Pd-(Ar-BIP) catalysts show a good affinity for the polar monomer, a good thermal stability and favor the cleavage of the catalyst resting state, leading to copolymer with M_w values higher than that of the macromolecules produced with the corresponding Pd-(Ar-BIAN) under the same reaction conditions. NMR characterization of the produced copolymers points out that the polar monomer is inserted both at the end of the branches and into the main chain, with a more selective enchainment than that achieved when the copolymerization is carried out in dichloromethane. In situ NMR investigations allowed us to detect relevant intermediates of the catalytic cycle and shed light on the nature of possible deactivation species.

Introduction

Functionalized polyolefins are highly desirable materials that are currently produced by industrial processes based on radical reactions, which suffer from low cost efficiency, high energy consumption and a poor control over the macromolecule structure. The direct, controlled, homogeneously catalyzed copolymerization of ethylene with polar vinyl monomers represents the most powerful and environmentally friendly approach to overcome these limits.¹

The breakthrough in the field is represented by Brookhart's catalytic system based on Pd(II) complexes with α -diimine (N-N) molecules characterized by either the acenaphthene (Ar-BIAN) or the 1,4-diaza-1,3-butadiene skeleton (Ar-DAB) (Chart 1).² This catalytic system was the first able to copolymerize ethylene with acrylic esters, like methyl acrylate (MA), yielding the real copolymer with the polar monomer inserted into the branches of the macromolecule. A few years later, Pugh reported the in situ Pd(II) catalytic system based on a phosphino-sulfonate (P-O) ligand (Chart 1).³ The two systems show different activity in the production of ethylene/methyl acrylate copolymers having different molecular weight, amount of incorporated polar monomer and microstructures: branched macromolecules with the polar monomer at the end of the branches are obtained when the Pd-(N-N) system is applied, whereas linear macromolecules with the polar monomer into the main chain are the product of the Pd-(P-O) catalyst.

Chart 1. General structures of Pd-catalysts with different ligands.

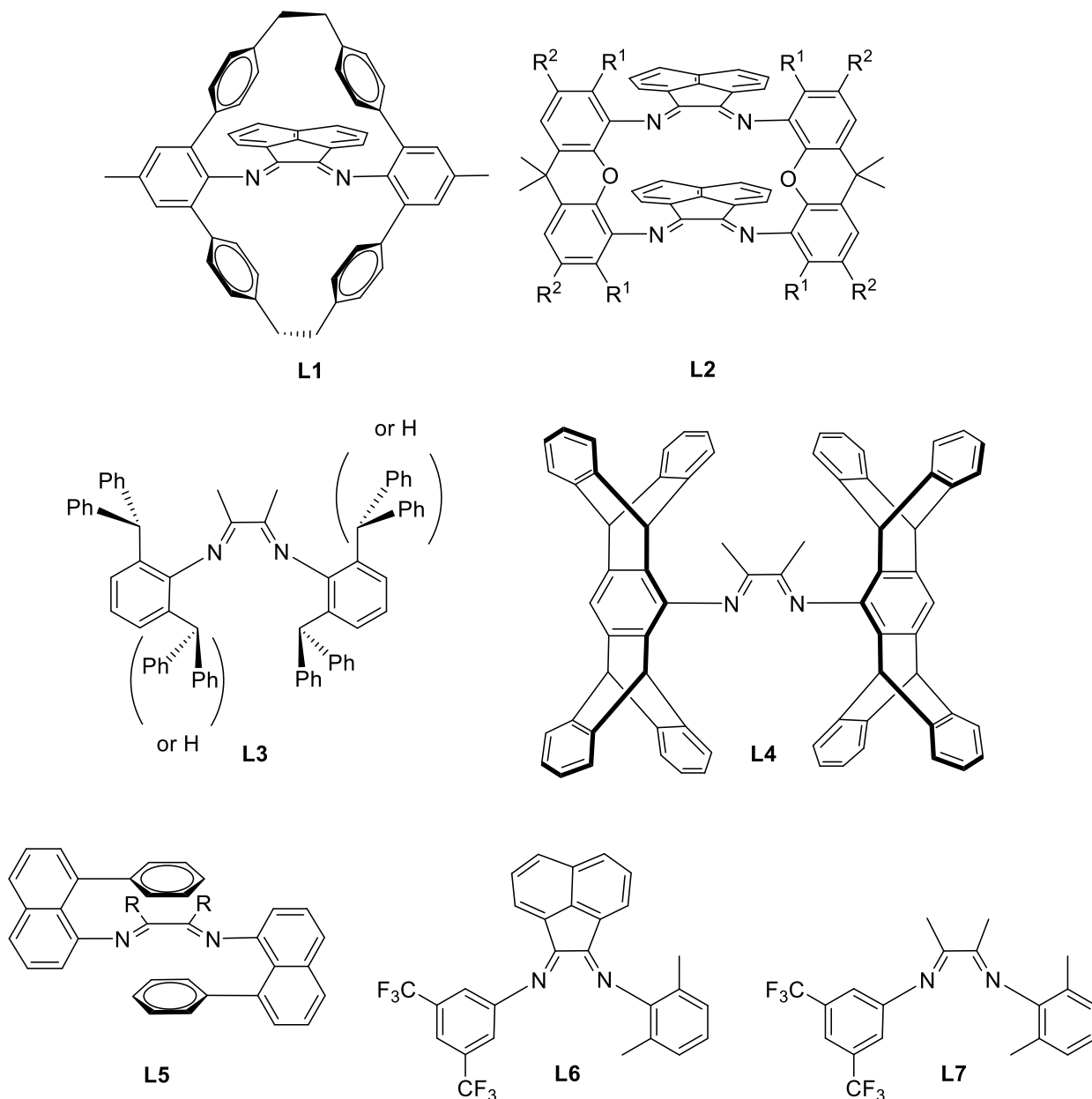


These two catalytic systems remained the only ones to be investigated for almost two decades and only recently other ancillary ligands have been considered (Chart 1), like bisphosphine monoxide (BPMO),⁴ N-heterocyclic carbene-quinolinolate (IzQO),⁵ and N-heterocyclic carbene-phosphine oxide (NCPO) ligands,⁶ phosphonic diamide phosphines (PDAP)⁷ and amine-imine derivatives.⁸

Even though DFT calculation indicated palladium as the most suitable transition metal to obtain catalysts for the ethylene/polar vinyl monomer copolymerization,⁹ in the last two years a few examples based on Ni(II) appeared.¹⁰

Focusing the attention on Pd(II) catalysts with α -diimine ligands, most of the studies deal with the variation of the substituents on the aryl rings. As a few examples to be mentioned, we consider a cyclophane based α -diimine (**L1** in Chart 2), whose corresponding catalyst has an enhanced life-time leading to a copolymer with a higher content of MA with respect to the acyclic analogue;¹¹ a dinuclear catalyst based on a macrocyclic α -diimine (**L2** in Chart 2) that leads to a copolymer with the polar monomer located both in the main chain and at the end of the branches;¹² di- or monophenylmethyl substituted α -diimines (**L3** in Chart 2), whose corresponding catalysts are highly robust and lead to ethylene/MA copolymers with high molecular weight and low branching density;¹³ the corresponding rotationally restricted pentiptycenylyl N-aryl substituted diimine, whose Pd(II) catalyst shows an enhanced comonomer incorporation (**L4** in Chart 2);¹⁴ the bulky 8-*p*-tolyl naphthyl substituted α -diimine (**L5** in Chart 2), whose relevant Pd complex catalyzes the living copolymerization of ethylene with methyl acrylate.¹⁵ Some of us introduced Pd-catalysts based on nonsymmetrical α -diimines with either a BIAN or a DAB skeleton (**L6** and **L7** in Chart 2). Depending on the substituents of the aryl rings better performing catalysts are obtained with respect to those having the corresponding symmetrical ligands.¹⁶

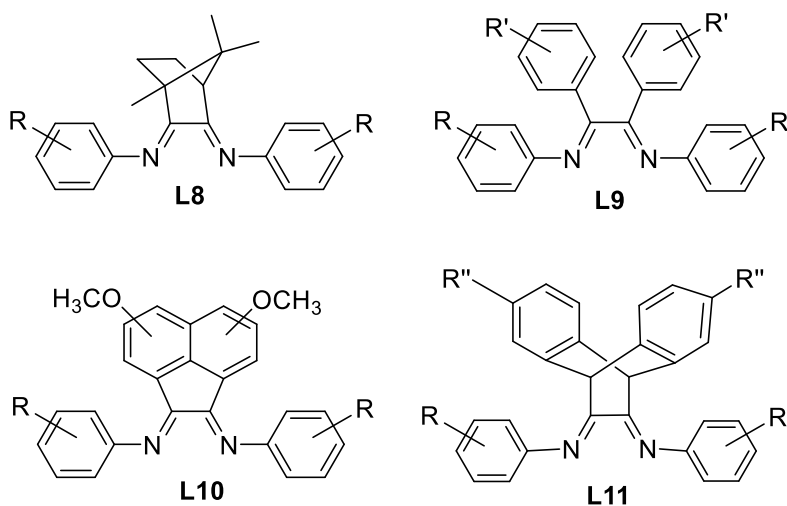
Chart 2. Examples of reported α -diimine ligands.



On the contrary, studies about the variations of the ligand backbone are much more limited. α -Diimines with either a camphyl or two phenyls or substituted phenyl rings have been considered (**L8** and **L9** in Chart 3).¹⁷ The catalytic performances of the relevant palladium complexes remarkably depend on the ligand skeleton. The catalysts with the ligand having the aryl

substituted skeleton showed a great drop in both catalytic activity and incorporation of MA, whereas the camphyl α -diimine based catalyst afforded high molecular weight ethylene/MA copolymers with high incorporation of MA, even though with lower TOF with respect to the Brookhart's type catalyst. The introduction of methoxy groups on the acenaphthene skeleton (**L10** in Chart 3) resulted in Pd(II) catalysts with higher activity than that of the Brookhart's type catalyst and yielding the copolymer with a higher molecular weight.¹⁸ Finally, an α -diimine with a substituted dibenzobarrelene skeleton was used to synthesize both palladium(II)¹⁹ and nickel(II) complexes. The latter demonstrated to be catalysts for the copolymerization of ethylene with methyl 10-undecenoate (**L11** in Chart 3).^{10a}

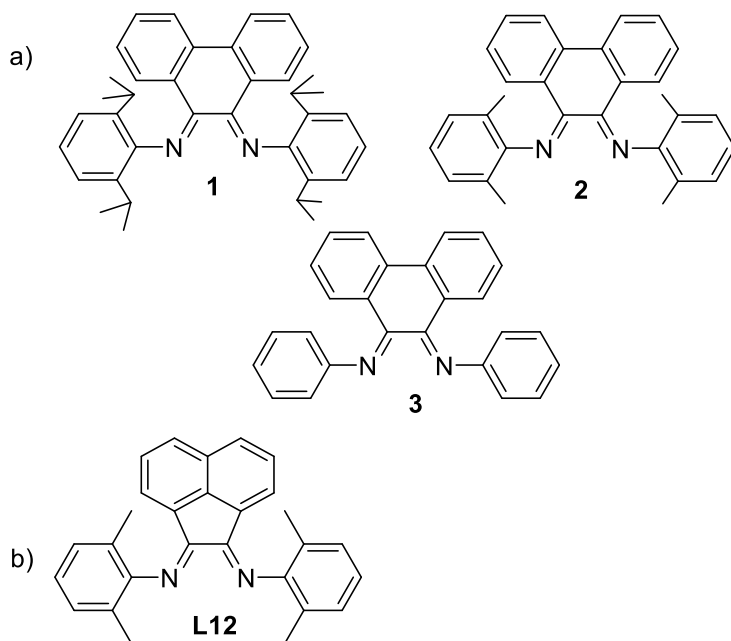
Chart 3. α -Diimines with different backbones.



In this work we have studied the catalytic behavior of organometallic palladium(II) complexes based on α -diimine ligands featuring a phenanthrene skeleton (Ar-BIP). The ligands of choice have the aryl rings substituted in 2,6-positions with either a methyl or an isopropyl group,

whereas the molecule with the simple phenyl was considered as a reference compound (Ligands **1-3** in Chart 4).

Chart 4. α -Diimines under investigation.^a



^aa) Ar-BIP molecules; b) already reported α -diimine.

The coordination chemistry of ligands **1-3** to Pd(II) has been investigated in detail pointing out remarkable differences with respect to that of the corresponding Ar-BIAN molecules. Neutral, $[\text{Pd}(\text{Ar-BIP})(\text{CH}_3)\text{Cl}]$, and monocationic, $[\text{Pd}(\text{Ar-BIP})(\text{CH}_3)(\text{NCCH}_3)][\text{PF}_6]$, complexes were studied. The latter were applied as precatalysts in the ethylene/methyl acrylate copolymerization reaction and the catalytic behavior compared to that of the catalysts having the corresponding Ar-BIAN. *In situ* NMR investigations about the reactivity of the monocationic complexes with methyl acrylate allowed us to shed light on the possible catalyst deactivation forms.

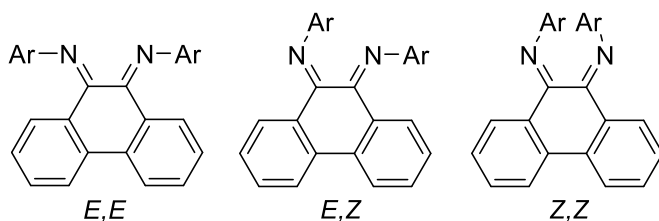
Results and discussion

Synthesis and Characterization of Ar-BIP ligands and the relevant Pd(II) complexes

Ar-BIP molecules were reported for the first time in 1996 by Elsevier,²⁰ and have been recently reconsidered as ancillary ligands for catalysts for ring-opening polymerization of *rac*-lactides,²¹ ethylene polymerization,^{21b} and isoprene polymerization.^{21c}

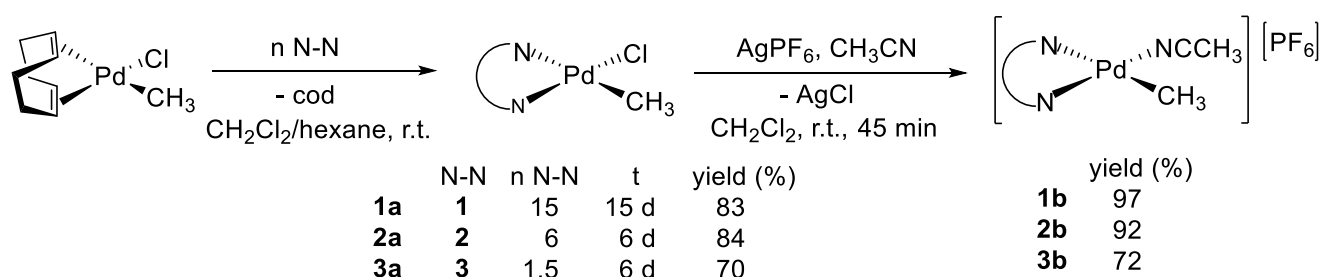
Of the three different synthetic methodologies present in the literature, only the one based on the reaction of 9,10-phenanthrenequinone with the desired aniline, at room temperature, in the presence of TiCl₄, resulted to be successful in our hands.²² Ligands **1-3**, isolated in moderate yields (40 – 60 %) as solids of orange (**1**, **2**) or red (**3**) color, were characterized by mass spectrometry and NMR spectroscopy in solution. In analogy to Ar-BIAN molecules, also for Ar-BIPs *E,Z*, *E,E*, and *Z,Z* isomers are possible depending on the relative configuration of the aryl rings with respect to the C=N imine bonds (Chart 5). In agreement with literature, in the ¹H NMR spectra of **1** and **2**, recorded in CD₂Cl₂ at 298 K, the number of signals and their integration indicated the presence of the nonsymmetrical *E,Z* isomer,^{21b, 21c, 22} whereas for **3** the symmetrical *Z,Z* isomer was present.²⁰⁻²¹ This represents a first main difference with respect to Ar-BIANs: these latter are always present in solution as a mixture of *E,Z* and *E,E* isomers, in equilibrium at slow rate on the NMR timescale. The *Z,Z* isomer was never observed up to now.^{16a, 16c, 20, 23}

Chart 5. *E,E*, *E,Z*, and *Z,Z* isomers for Ar-BIP ligands.



Ligands **1-3** were used to synthesize the corresponding neutral, $[\text{Pd}(\text{Ar-BIP})(\text{CH}_3)\text{Cl}]$ **1a – 3a**, and monocationic, $[\text{Pd}(\text{Ar-BIP})(\text{CH}_3)(\text{NCCH}_3)][\text{PF}_6]$ **1b – 3b**, organometallic Pd(II) complexes. The synthetic procedure applied to obtain the neutral derivatives, **1a – 3a**, was based on the well known substitution reaction of cyclooctadiene with α -diimine on the palladium precursor $[\text{Pd}(\text{cod})(\text{CH}_3)\text{Cl}]$ (cod = 1,5-*cis,cis*-cyclooctadiene).²⁴ However, unlike the facile synthesis of organometallic Pd(II) complexes with the corresponding Ar-BIANs, namely $[\text{Pd}(\text{Ar-BIAN})(\text{CH}_3)\text{Cl}]$, much longer reaction times (up to 15 days) and larger excess of ligands with respect to palladium (up to 15 equiv.) were required to obtain the neutral complexes **1a – 3a** (Scheme 1).

Scheme 1. Synthesis of Pd(II) Complexes



Long reaction times were previously reported for the synthesis of analogous palladium(II) complexes with either the 8-*p*-tolyl-naphthyl or 2,6-bis(diphenylmethyl)-4-methyl substituted Ar-

BIAN or Ar-DAB imines,^{13a, 15} due to the bulkiness of the ligand. In the case under investigation, the difficulties in the coordination to palladium(II) of Ar-BIP molecules might be ascribed to two main factors: *i.* the lack in solution of the *E,E* species, that is the geometrical isomer required for coordination of Ar-BIP to the metal center as a chelating ligand. Therefore, an isomerization process has to occur before coordination. For Ar-BIANs in solution the isomerization from *E,Z* to *E,E* isomer is very easy,^{23c} but apparently this is not the case for Ar-BIPs; *ii.* the structure of ligands **1-3** in solid state points out that, unlike the Ar-BIANs, both the phenanthrene skeleton and the iminic fragment NCCN are not planar, for the latter the torsion angles are of 44.3(4), 45.0(1) and 44.7(5)°, for **1**,^{21c} **2**,²² and **3**,²⁰ respectively (Table 1). This torsion angle must remarkably decrease for the coordination of Ar-BIP as a chelating ligand to palladium leading to a square planar complex. In addition, for ligands **1** and **2**, the steric hindrance of the substituents in *ortho* positions of the aryl rings might also disfavor the coordination. Nevertheless, by following our synthetic methodology, complexes **1a** – **3a** were isolated as dark purple solids in good to high yields (70 - 84 %). The monocationic derivatives **1b** – **3b** were obtained in high yield from the neutral precursors **1a** – **3a** by following the reported synthetic procedure^{24b} with no difficulties, confirming that the bottleneck in the synthesis of the neutral complexes is the coordination of Ar-BIPs to palladium.

Single crystals suitable for X-ray analysis of **2a** and **3a** were obtained by slow diffusion of *n*-hexane into a dichloromethane solution at 277 K (Figure 1).

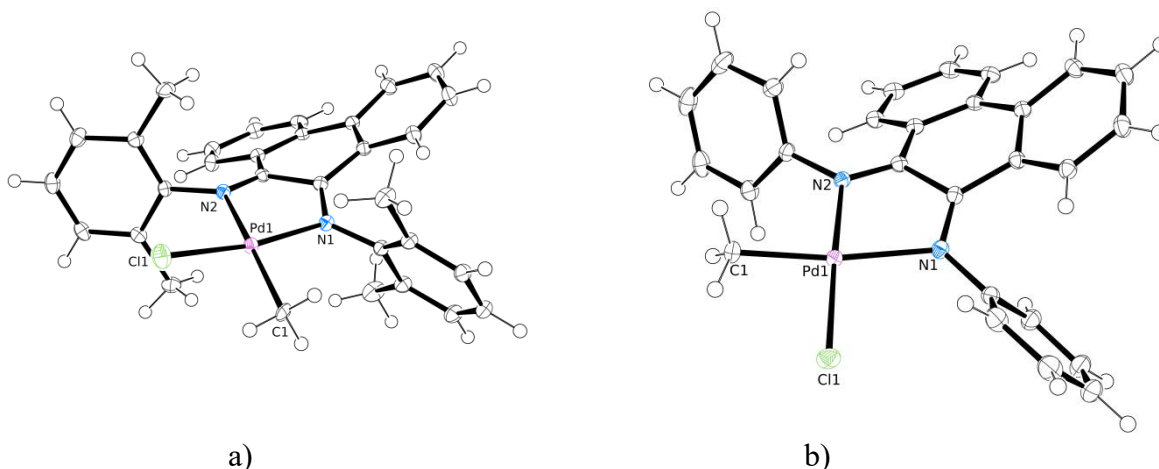
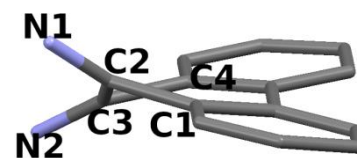


Figure 1. ORTEP drawing (50 % probability ellipsoids) for complexes: a) **2a**; b) **3a**. Selected bond lengths (Å) and angles (°) for: **2a** Pd(1)-N(1) 2.064(1), Pd(1)-N(2) 2.122(1), Pd(1)-C 2.087(2), Pd(1)-Cl(1) 2.2821(5), N(1)-Pd(1)-N(2) 77.38(5), C(1)-Pd(1)-Cl(1) 85.64(6), N(1)-Pd(1)-C(1) 99.41(7), N(2)-Pd(1)-Cl(1) 98.73(4); **3a** Pd(1)-N(2) 2.043(1), Pd(1)-N(1) 2.171(1), Pd(1)-C(1) 2.035(1), Pd(1)-Cl(1) 2.2924(5), N(2)-Pd(1)-N(1) 76.99(4), C(1)-Pd(1)-Cl(1) 86.29(4), C(1)-Pd(1)-N(2) 96.08(5), N(1)-Pd(1)-Cl(1) 100.93(3).

The structural analysis indicates that the coordination of the Ar-BIP ligands to the Pd center decreases their configurational freedom due to the constraint of a square planar geometry. This is reflected by the substantial decrease of the NCCN and CCCC torsion angles as well as the NCC angles of the diiminic fragment upon coordination (Table 1).

Table 1. NCC angles, NCCN and CCCC torsion angles (in degrees, as defined by the schematic drawing) for free and coordinated **2** and **3** ligands; for comparison purposes, the data for the Ar-BIAN counterpart of complex **2a**, **L12a**, have also been included; standard deviations (where available) are in parentheses.

Cmpnd	N ₁ C ₂ C ₃	N ₂ C ₃ C ₂	N ₁ C ₂ C ₃ N ₂	C ₁ C ₂ C ₃ C ₄
2	115.8	126.11	45.0(1)	41.3
2a	115.1(1)	113.6(1)	22.0(2)	29.6(2)
L12a	118.4	119.0	4.1	0.7
3	117.2	126.33	44.7(5)	47.4
3a	114.3(1)	115.1(1)	21.3(1)	32.9(2)



The solid state structure of complex **2a** can be compared with that of its Ar-BIAN counterpart, [Pd(**L12**)(CH₃)Cl], **L12a**.²⁵ In complex **2a** both Pd-N bond distances are shorter than those in **L12a** (2.064(1) and 2.122(1) Å in **2a** vs 2.088(6) and 2.203(5) Å in **L12a**), indicating a stronger coordination of the Ar-BIP ligand with respect to the Ar-BIAN molecule. This trend is reflected by the value of the Pd-C bond length that is longer in **2a** (2.087(2) Å) than in **L12a** (2.039(6) Å). Another evident difference is in the degree of planarity of the diiminic moiety, the Ar-BIAN ligand being almost perfectly planar, while the Ar-BIP molecule being markedly twisted (Table 1, Figure 2a). A greater strain in the Ar-BIP derivative is also indicated by the NCC angles, which are nearly ideal for **L12a**, while they are substantially lower than 120° for **2a** (Table 1). As a consequence, the N-Ph bonds in **2a** are bent away from the diazo ligand as compared to **L12a**. This effect is measured by the angle between the N-Ph bond and the line passing through the Pd atom and bisecting the opposite C-C bond (Figure 2b): the values for each N-Ph bond in **2a** and **L12a** are 80.3°, 80.8° and 88.1°, 86.7°, respectively.

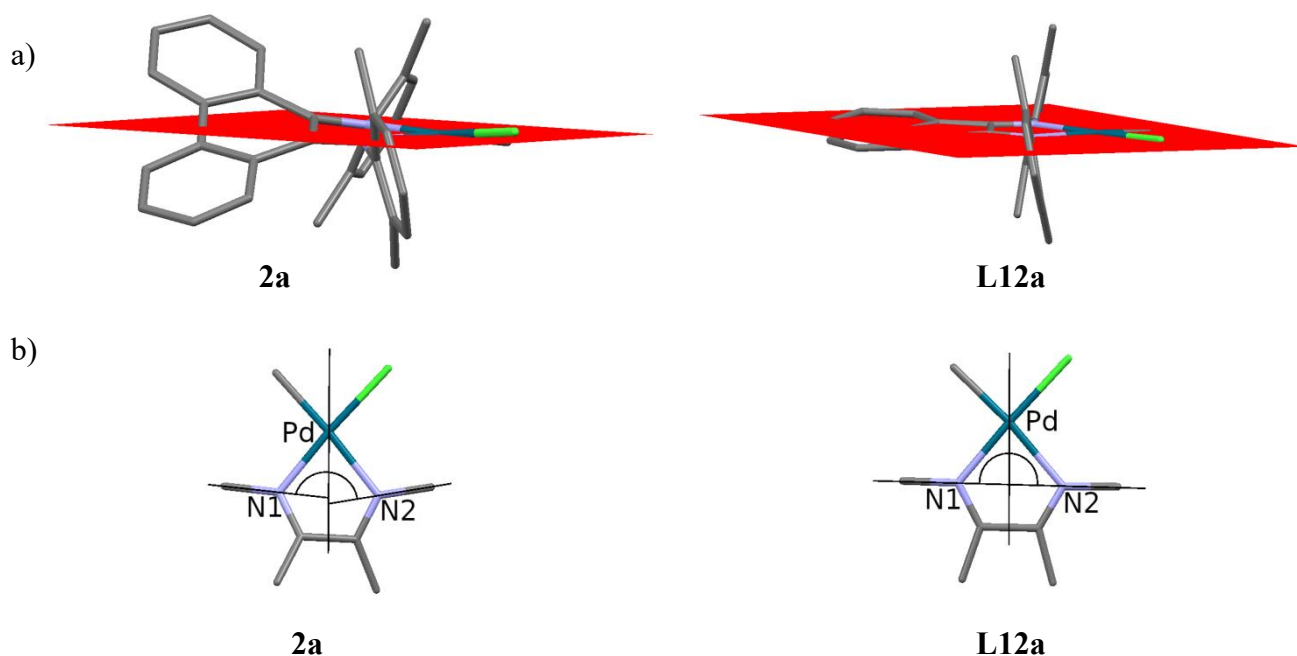


Figure 2. a) Average plane through the Pd and the four atoms directly bonded to it in complex **2a** and **L12a** to evidence the different degree of planarity of the diiminic ligand; b) Schematic drawing showing the bending effect on the N-Ph bonds in **2a** as compared to **L12a**.

Both neutral and monocationic complexes were characterized in solution by NMR spectroscopy recording the spectra in CD_2Cl_2 at 263 K and in CDCl_3 at 298 K, respectively. In the ^1H NMR spectra the number of signals and their integration are in agreement with the coordination of the ligand in a nonsymmetric chemical environment. The singlet of the Pd- CH_3 fragment falls between 0.78 and 0.41 ppm for the neutral complexes and between 0.88 and 0.50 ppm for the monocationic derivatives. In the ^1H NMR spectra of **L12a** and $[\text{Pd}(\text{L12})(\text{CH}_3)(\text{NCCH}_3)][\text{PF}_6]$ **L12b**, the Pd- CH_3 moiety resonates at 0.61 and 0.73 ppm, respectively, that is at higher frequency than the same signal for **2a** and **2b** (0.32 and 0.42 ppm). According to our hypothesis that this signal might be considered as a good probe for assessing

the electron density donated by the ligand to the metal center,^{16, 26} the variation in its chemical shift moving from Ar-BIAN to Ar-BIP complexes indicates that **2** has a higher Lewis basicity than **L12**. This is in agreement with the trend of the Pd-N bond distances measured in solid state (Figure 1) and might be related to the lack of conjugation between the two C=N bonds in the free ligand.²⁰ These trends suggest that Ar-BIPs are stronger ligands than Ar-BIANs, and, in analogy with the study on the Pd-PDAP ligand,⁷ the Pd-(Ar-BIP) cationic complexes can be considered as electron-rich metal cations.

Ethylene/methyl acrylate copolymerization

Complexes **1b** – **3b** were tested as precatalysts for the ethylene/methyl acrylate copolymerization (Scheme 2, Table 2) by carrying out the reaction in 2,2,2-trifluoroethanol at mild reaction conditions of temperature and ethylene pressure and with no addition of any cocatalyst. The same reaction conditions were applied for the complex with ligand **L12**, in order to have a direct comparison of data.

Before workup, a sample for GC-MS was taken in order to analyze the presence of alkene oligomers. The catalytic products were isolated as brown oils and characterized by NMR spectroscopy after removal of the volatile fraction at reduced pressure (Figure S45-S54). The molecular weight of the produced macromolecules was determined by GPC analysis.

Scheme 2. Ethylene/methyl acrylate copolymerization.

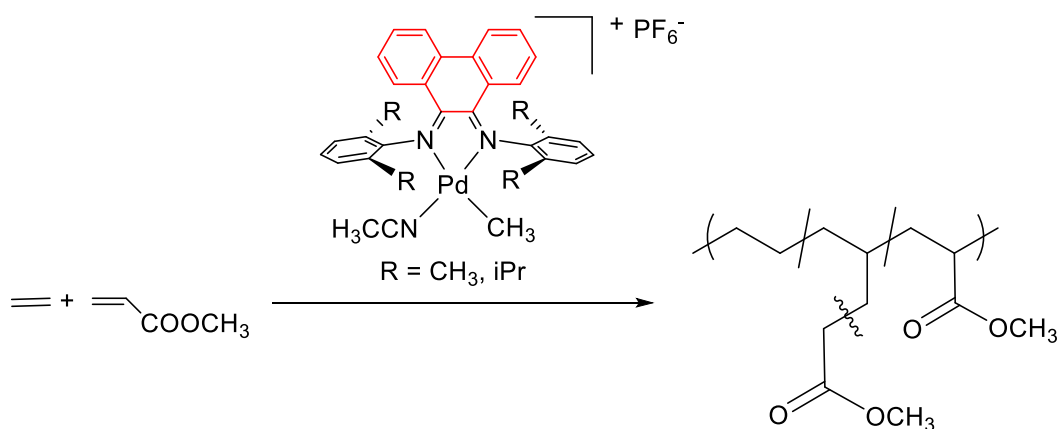


Table 2. Ethylene/methyl acrylate copolymerization: effect of the ancillary ligand.^[a]

Run	PreCat	Yield (mg)	g CP/ mol Pd ^[b]	MA (mol %) ^[c]	TON ^[d]		Mn (Mw/Mn) ^[e]	Alkenes /esters ^[f]	Bd ^[c, i]
					E	MA			
1	1b	436.4	20781	0.3	734	2.21	33000 (1.54)	none	83
2	2b	156.6	7443	2.4	248	6.08	10000 (1.60)	none	103
3	3b	-	-	-	-	-	-	C ₄	-
4	L12b	379.3	18062	4.4	564	26.0	3200 (2.06)	none	111
5 ^[g]	1b	452.1	21529	-	767		23000 (2.66)	none	90
6 ^[g]	2b	181.7	8652	-	308		7800 (1.80)	none	114

^[a] Reaction conditions: precatalyst [Pd(CH₃)(NCCH₃)(N-N)][PF₆], n_{Pd} = 2.1 · 10⁻⁵ mol, V_{TFE} = 21 mL, V_{MA} = 1.130 mL, [MA]/[Pd] = 594, T = 308 K, P_{ethylene} = 2.5 bar, t = 18 h; ^[b] isolated yield, productivity as g CP/mol Pd = grams of copolymer per mole of palladium; ^[c] calculated by ¹H NMR spectroscopy on isolated product; ^[d] Turnover number = mol of substrate converted per mol of catalyst (E = ethylene); ^[e] determined by GPC at 30 °C, using THF as the solvent, an eluent flow rate of 1 mL min⁻¹, and 19 narrow polystyrene standards as the reference; ^[f] determined by GC/MS; ^[g] Reaction conditions: n_{Pd} = 2.1 · 10⁻⁵ mol, V_{TFE} = 21 mL, T = 308 K,

$P_{\text{ethylene}} = 2.5 \text{ bar}$, $t = 18 \text{ h}$; ^[h] n.d. = not determined; ^[i] Bd = degree of branching as branches per 1000 carbon atoms.

A remarkable effect of the N-donor ligand on the catalytic behavior is observed, comparing both the phenanthrene-based ligands bearing different substituents on the aryl ring and ligands with a different backbone (Table 2). Inside the series of complexes with Ar-BIP ligands, **3b** is found to be inactive towards the copolymerization reaction, yielding only a mixture of butenes (Table 2, run 3). Complexes with the *ortho*-substituted Ar-BIP, **1b** and **2b**, generate active catalysts leading to the formation of ethylene/MA copolymers. An increase in the productivity is achieved on going from the catalyst with the methyl-substituted Ar-BIP, **2**, to that with the isopropyl-substituted ligand, **1**, and the highest value of productivity is reached with precatalyst **1b** (almost 21 kg CP/mol Pd, Table 2, run 1). The different substitution on the aryl rings also affects the content of inserted polar monomer, the molecular weight and the branching degree of the copolymers: the first feature remarkably decreases on going from catalyst with **2** to that with **1**, whereas the second parameter increases of three times following the same order and an M_n of 33000 is reached, together with a decrease of branching degree (Table 2, runs 1, 2). In both cases no formation of alkene oligomers was observed, as expected for catalysts having hindered apical positions around the metal center.^{1k, 27} Despite the different reaction conditions, the trends observed moving from **2b** to **1b** are similar to those reported for Ar-DAB catalysts, and are mainly related to the different steric hindrance around the catalytic center.^{2b} However, whereas for the Ar-DAB catalysts TON decreases for both comonomers when going from the iso-propyl substituted ligand to the methyl derivative,^{2b} for the Ar-BIP catalysts an increase in the TON of the polar monomer is found. Precatalysts **1b** and **2b** are also found active in ethylene homopolymerization (Table 2, runs 5 and 6), but the increase in the productivity with respect to

the ethylene/MA copolymerization is not as pronounced as that reported in the literature for Ar-DAB catalysts (where the difference is of one order of magnitude).^{2a} It is accepted that the low productivity in the copolymerization with respect to ethylene homopolymerization is due to the formation of the stable six-membered palladacycle (species C" in Scheme 3), which inhibits the subsequent alkene insertion and represents the catalyst resting state.^{2b} Therefore, the small difference in productivity observed for the Ar-BIP catalysts in the two polymerizations suggests a lower stability of the metallacycle C", that easily cleaves favoring the growth of the polymer chain. This is in agreement with the higher Lewis basicity of the Ar-BIP ligands that makes the palladium center less oxophilic, disfavoring the formation of the Pd-O bond in C". In addition, in literature the Ar-DAB catalysts are applied for the ethylene homopolymerization in dichloromethane, whereas here the Ar-BIP derivatives are tested in trifluoroethanol, a solvent never used for polyolefin synthesis. Due to the remarkably different nature of the two solvents, it cannot be ruled out that trifluoroethanol plays a role in determining catalyst productivity.

The direct comparison with the catalytic behavior of **L12b** points out that the Ar-BIAN catalyst is more productive than the active species with the corresponding Ar-BIP **2** and yields a copolymer with a higher content of polar monomer, but with three times lower molecular weight value and a slightly higher branching degree (Table 2, runs 2 and 4). The lower content of inserted polar monomer in the macromolecules produced with **2b** might be related to the additional bulkiness around palladium created by the phenanthrene skeleton, as evidenced by the X-ray analysis (Figure 2a). This higher steric congestion might be also responsible for the higher molecular weight of the produced copolymers. In addition, as recently reported for the Pd-PDAP catalysts,⁷ also the higher Lewis basicity of Ar-BIP ligands with respect to the corresponding Ar-BIAN derivatives can play a positive role in enhancing the length of polymer chains.

The influence of catalytic parameters, like temperature, ethylene pressure, methyl acrylate to palladium ratio, and reaction time has been evaluated for precatalysts **1b** and **2b**, in order to optimize the system. As a general observation, in the investigated ranges complex **2b** is more affected than **1b** by the parameter variations.

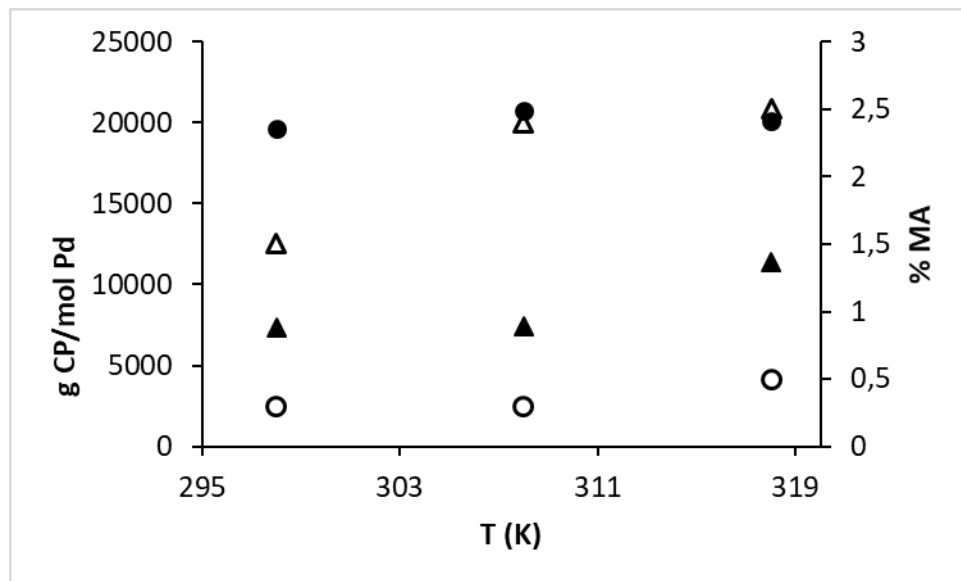


Figure 3. Ethylene/methyl acrylate copolymerization: effect of temperature. Precatalyst: $[\text{Pd}(\text{Ar-BIP})(\text{CH}_3)(\text{CH}_3\text{CN})][\text{PF}_6]$ (Ar-BIP = **1**, **2**). Reaction conditions: see Table 2. Filled symbols: productivity data; open symbols: content of MA in mol %; **1b** (\bullet, \circ), **2b** ($\blacktriangle, \triangle$).

The temperature influence was investigated in the range 298 - 318 K (Figure 3, Table S2). The catalytic performances of **1b**, in terms of productivity, content of inserted polar monomer and molecular weight, are almost unaffected by the temperature variation, whereas for **2b** a clear increase in both productivity and content of MA is observed, together with a decrease in the molecular weight (Table S2). This effect on MW indicates that the raise of productivity is related to an increase in the number of produced macromolecules rather than in their length, thus

suggesting that the decrease in the propagation to chain transfer rate ratio is due to an increase in the rate of the chain transfer step. The influence of temperature on the productivity represents a main difference with respect to the classical Ar-BIAN-based catalysts, whose productivity remarkably drops at 318 K due to the decomposition to inactive palladium metal.^{2a, 16a} The improved thermal stability of the Ar-BIP catalysts is in agreement with both the stronger coordinating capability of Ar-BIP ligands with respect to Ar-BIANs and the increase in the bulkiness of the ligand. The latter is a strategy already successfully applied in the Ni- and Pd-catalyzed ethylene homopolymerization,^{10a, 11a, 15, 17} and in one example of ethylene/MA copolymerization, where the increase in the content of inserted MA was achieved together with a decrease in the productivity when the reaction temperature was raised from 293 to 333 K.^{13a}

The effect of the ethylene pressure was studied in the range 2.5 - 7.0 bar. The increase in the ethylene pressure has no effect on the performance of the catalyst obtained from **1b** (Table S3, runs 1 - 3), whereas for **2b** the productivity almost doubles when the ethylene pressure is increased from 2.5 to 5.0 bar together with a drop in the content of the polar monomer (Table S3, run 4 vs 5). A further increase of ethylene pressure up to 7 bar results in a decrease in the productivity (Table S3). A similar effect of the ethylene pressure on the productivity was observed by us in the ethylene/MA cooligomerization catalyzed by Pd-complexes with the nonsymmetric BIAN **L6**, also carried out in trifluoroethanol.^{16a} For the catalysts under investigation the effect is more pronounced and it might be related to the fact that, as reported in Table 2, the Ar-BIP complexes are not good catalysts for ethylene homopolymerization.

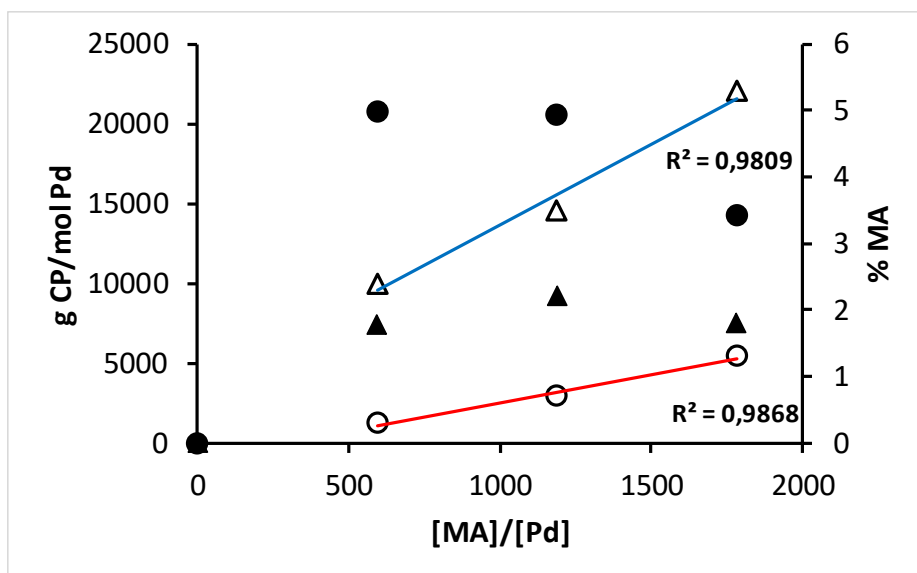


Figure 4. Ethylene/methyl acrylate copolymerization: effect of $[MA]/[Pd]$ ratio. Precatalyst: $[Pd(Ar-BIP)(CH_3)(CH_3CN)][PF_6]$ ($Ar-BIP = 1, 2$). Reaction conditions: see Table 2. Filled symbols: productivity data; open symbols: mol % MA; **1b** (\bullet, \circ), **2b** ($\blacktriangle, \triangle$).

The effect of methyl acrylate to palladium ratio was investigated by increasing the amount of the polar monomer in the range $[MA]/[Pd] = 594-1782$ and by keeping constant the amount of precatalyst. In agreement with the data on Ar-DAB catalysts,² the content of the inserted polar monomer linearly increases with MA concentration (Figure 4, Table S4). A concomitant decrease in the M_n values is observed (Table S4). The effect on the productivity is different depending on Ar-BIP: for precatalyst **1b** a decrease in productivity is found due to a drop in ethylene turnover number; instead for **2b** an increase in the productivity associated with an increase in the values of TON for both comonomers is initially observed, followed by a decrease for a further increase of the $[MA]/[Pd]$ ratio (Table S4). Unlike the Ar-DAB catalysts,² for both precatalysts the turnover number for MA increases with the MA concentration, thus suggesting a higher affinity for the polar monomer of the Ar-BIP catalysts than of the Ar-BIAN derivatives,

and this might be related to the higher Lewis basicity of Ar-BIP, supporting the positive effect of having electron-rich metal cationic catalysts. This is also in agreement with DFT calculations showing that anionic Pd(II) catalysts are highly tolerant toward polar monomers.²⁸

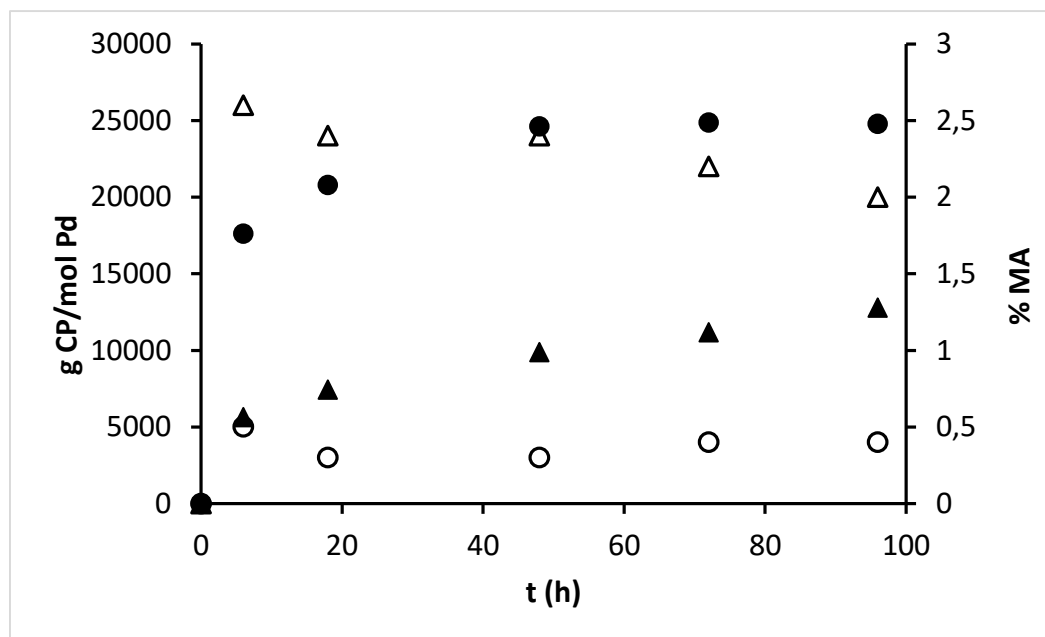


Figure 5. Ethylene/methyl acrylate copolymerization: effect of reaction time. Precatalyst: $[\text{Pd}(\text{Ar-BIP})(\text{CH}_3)(\text{CH}_3\text{CN})][\text{PF}_6]$ (Ar-BIP = **1**, **2**). Reaction conditions: see Table 2. Filled symbols: productivity data; open symbols: mol % MA; **1b** (●,○), **2b** (▲,△).

The catalytic behavior of precatalysts **1b** and **2b** was also assessed over time, in the range $t = 6 - 96$ hours, by carrying out the catalytic experiments at $P_E = 2.5$ bar and $T = 308$ K. Precatalyst **1b** is active up to 48 h, whereas **2b** is still working up to 96 h, reaching a productivity value of almost 25 and 13 kg CP/mol Pd, respectively (Figure 5, Table S5). In all the catalytic tests no formation of inactive palladium black was evident, indicating that catalyst deactivation follows a different mechanism than the decomposition to palladium metal implying ligand dissociation.

This is in agreement with the structural features of the complexes that indicate Ar-BIP molecules as stronger ligands to palladium than Ar-BIANs.

The increase in productivity with reaction time is related to the increase in turnover numbers for both comonomers, even though a slight decrease in the content of the inserted polar monomer is measured at longer reaction times for copolymers produced with **2b** (Figure 5, Table S5). The molecular weight increases during the first 18 h, levelling off afterwards, indicating that the increase in productivity is associated with the formation of more polymer chains rather than longer macromolecules.

Two selected catalytic experiments were performed by using a mass flow control device to measure the ethylene consumption (Figure 6). The catalysts obtained from **1b** and **2b** show similar kinetic profiles: *i.* an induction period of 90 s is observed; *ii.* the rate of ethylene uptake is the same up to 240 s; *iii.* afterward catalyst with **2** slows down, whereas catalyst with **1** is very active up to 2 h. Monitoring the ethylene consumption for 18 h, the deactivation of catalyst with ligand **1** becomes evident, while catalyst with ligand **2** remains active.

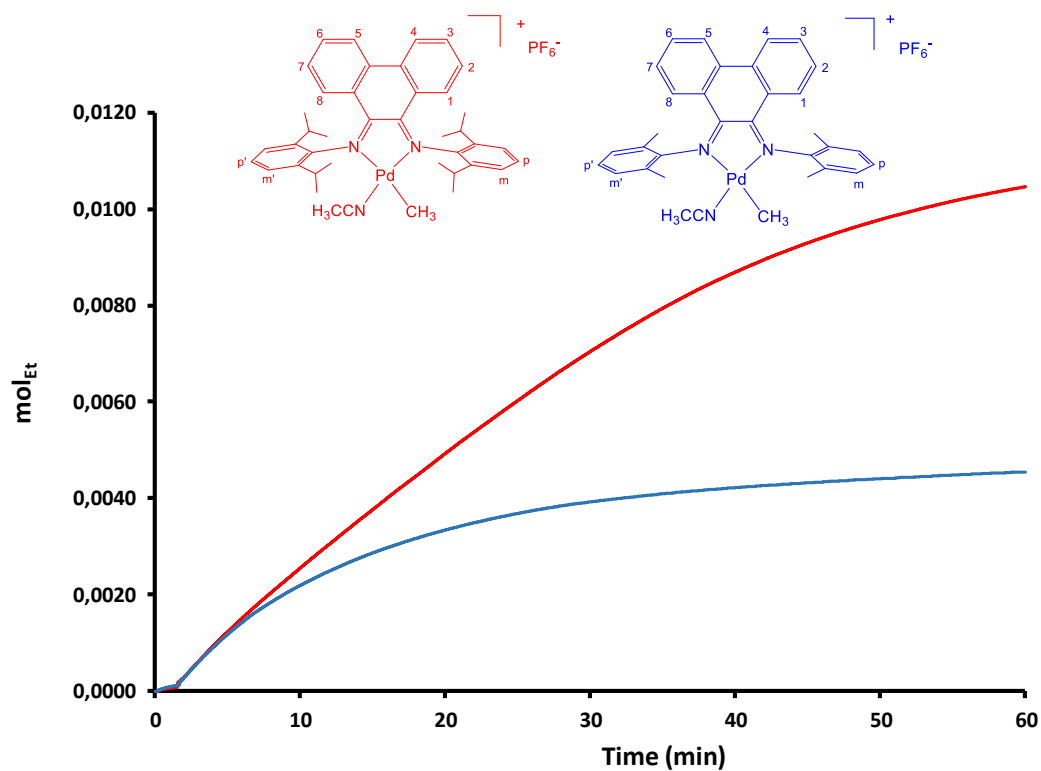
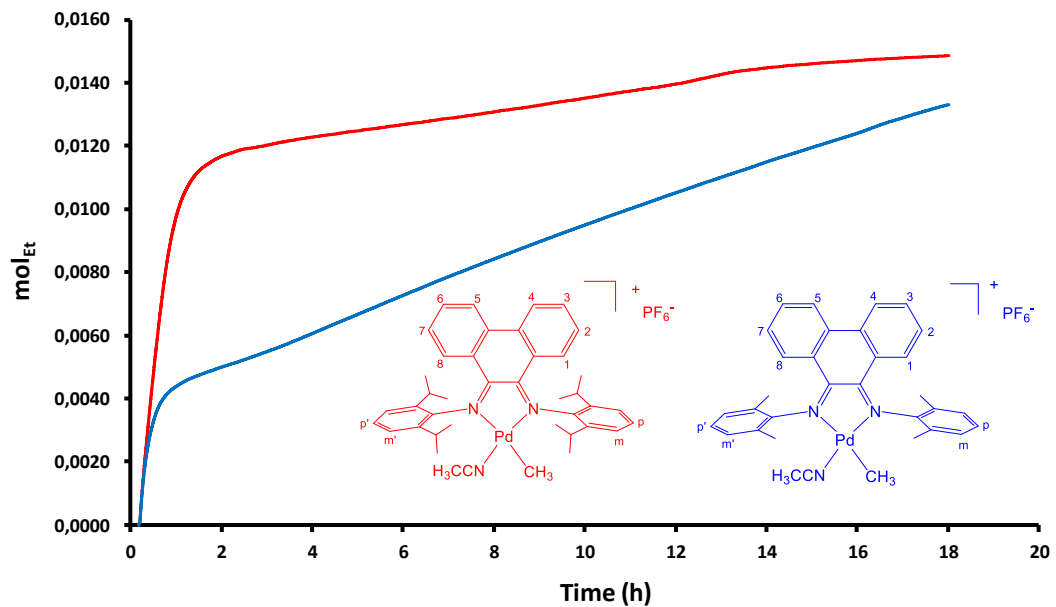


Figure 6. Ethylene/methyl acrylate copolymerization: kinetic profiles. Precatalyst: [Pd(Ar-BIP)(CH₃)(CH₃CN)]⁺[PF₆⁻] (Ar-BIP = **1** (red curve), **2** (blue curve)). Reaction conditions: see Table 2; up) ethylene uptake for 18 h; bottom) magnification of ethylene uptake in the time range: 0 – 1 h.

The characterization of the isolated catalytic product was performed by ^1H and ^{13}C NMR spectroscopy in CDCl_3 at room temperature. The signals in the ^1H NMR spectra were identified by comparison with literature data,^{2a, 3, 16a, 29} and assigned as follows: the singlet at 3.66 ppm to the methoxy group, the signals between 2.50 and 1.50 ppm to allylic protons and to methylenic groups closer to the ester functionality, the broad signal centred at 1.25 ppm to the methylenic and methinic moieties of ethylene units, and the signals between 1.0 and 0.6 ppm to methyl groups at the end of branches (Figure S45, S47). The signals due to the vinylic protons are not observed in the spectrum of the copolymer obtained with precatalyst **1b**, and signals of very low intensity are present in the spectrum of the copolymer produced with **2b**, in agreement with the polymeric nature of the catalytic product.

In the ^{13}C NMR spectra of the copolymers obtained with either **2b** or **L12b** (Table 2, run 2 and Table S5, run 11), in addition to the typical peaks of the methylenic and methyl groups, two overlapped signals for the methoxy (51.36 and 51.52 ppm) and one peak at 45.94 ppm are present. For the latter the $^1\text{H},^{13}\text{C}$ HSQC spectrum indicates its methinic nature. Three signals are present for the carbonyl group at 174.37, at 174.68 and 177.17 ppm. By comparison with the spectra reported in the literature for the ethylene/MA copolymers obtained with the Pd-(Ar-DAB) and the dinuclear Pd-(α -diimine) catalysts,^{2a, 12} the peak at 174.37 ppm is attributed to the acrylate units inserted at the end of the branches as the $-\text{CH}_2-\text{CH}_2-\text{C}(\text{O})\text{OCH}_3$ fragment. In agreement with the assignment of the ethylene/MA copolymers obtained with the Pd-**L2**-catalyst,¹² the signals at 177.17 and 45.94 ppm unambiguously indicate that the polar monomer is inserted into the main polymer chain (Figure 7). Inspection of the ^{13}C NMR spectrum of the copolymer obtained with **L12b** in CH_2Cl_2 , instead of TFE, shows the presence of the same

signals plus other two peaks for the carbonyl, at 177.23 and 167.07 ppm, respectively, that according to the literature,³⁰ are attributed to the polar monomer inserted at the beginning of the copolymer chain as $\text{CH}_3\text{-CH}(\text{CH}_2\text{COOCH}_3)\text{-CH}_2\text{-}$ fragment and at the end of the chain as an unsaturated moiety -CH=CH-COOCH_3 (Figure 7c). For the latter the methoxy peak at 3.69 ppm in the ^1H NMR spectrum is also observed (Figure S55). Thus, the NMR analysis indicates that when the copolymerization is carried out in trifluoroethanol the polar monomer is inserted in a more selective way than in dichloromethane and it is found both at the end of the branches and into the main chain, with a remarkable preference for the first kind of enchainment.

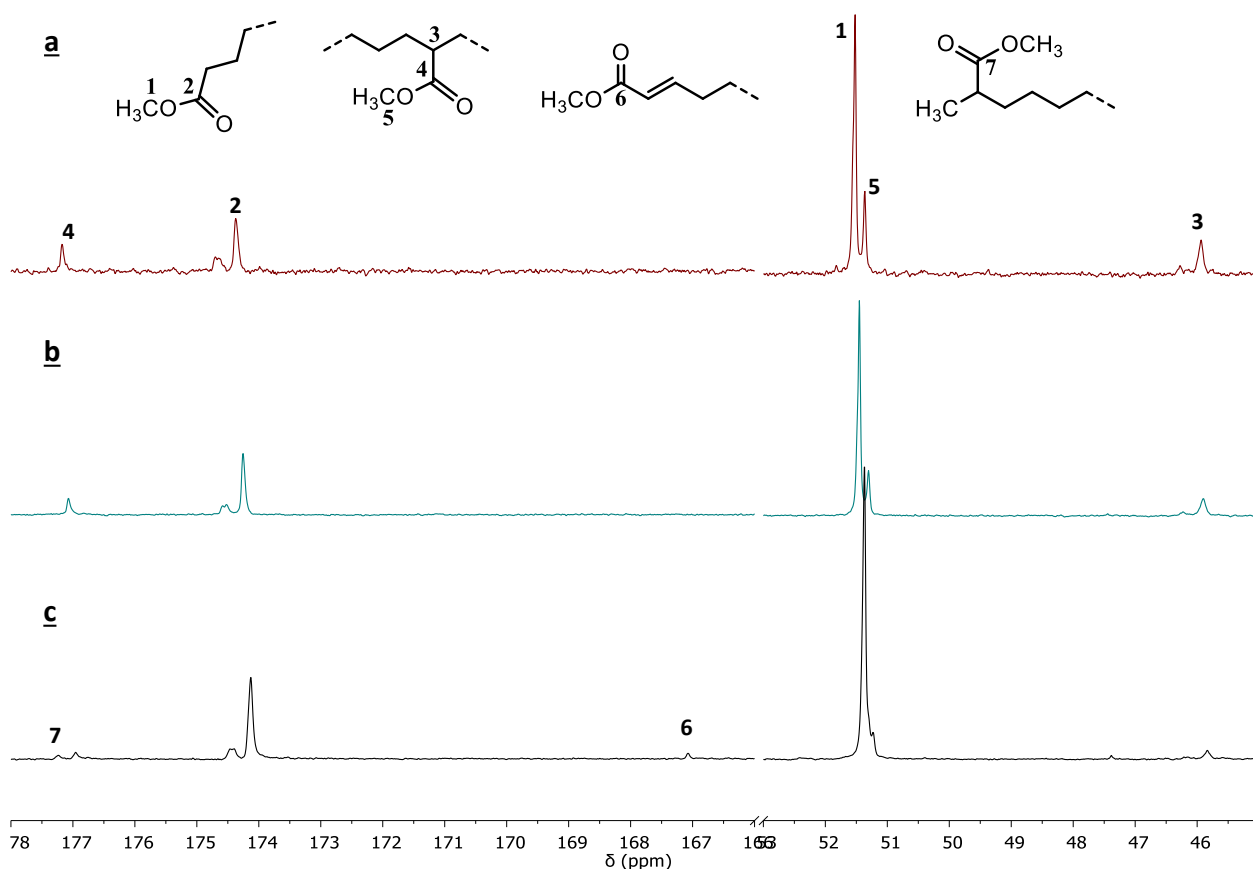


Figure 7. ^{13}C NMR spectra (CDCl_3 , 298 K) of ethylene/methyl acrylate copolymers synthesized with: a) **2b** in TFE; b) **L12b** in TFE; c) **L12b** in CH_2Cl_2 . Carbonyl region (left), methoxy and methinic region (right).

Whereas the beneficial effect of the fluorinated alcohol on the productivity was reported by some of us in the ethylene/MA copolymerization catalysed by Pd complexes with nonsymmetric α -diimines,^{16b, 16c} the solvent effect on the copolymer microstructure is evidenced here for the first time. It might be related to the fact that, thanks to its higher coordinating capability with respect to dichloromethane, trifluoroethanol favourably competes for the fourth coordination site on palladium that is necessary for β -hydrogen elimination to occur. Therefore, the latter is disfavored and, as a consequence, both termination and chain walking processes are inhibited leading to a more selective enchainment of MA. This hypothesis is in agreement with the molecular weight value, M_n , of the copolymers synthesized in the two solvents with **L12b**. The M_n value estimated by integration of the signals in the ^1H NMR spectra is 3200 and 2500 for the copolymer obtained in trifluoroethanol and dichloromethane, respectively.

In the ^{13}C NMR spectrum of the copolymers obtained with **1b** only the signals related to the polar monomer inserted at the end of the branches are evident (Figure S46).

Mechanistic investigation

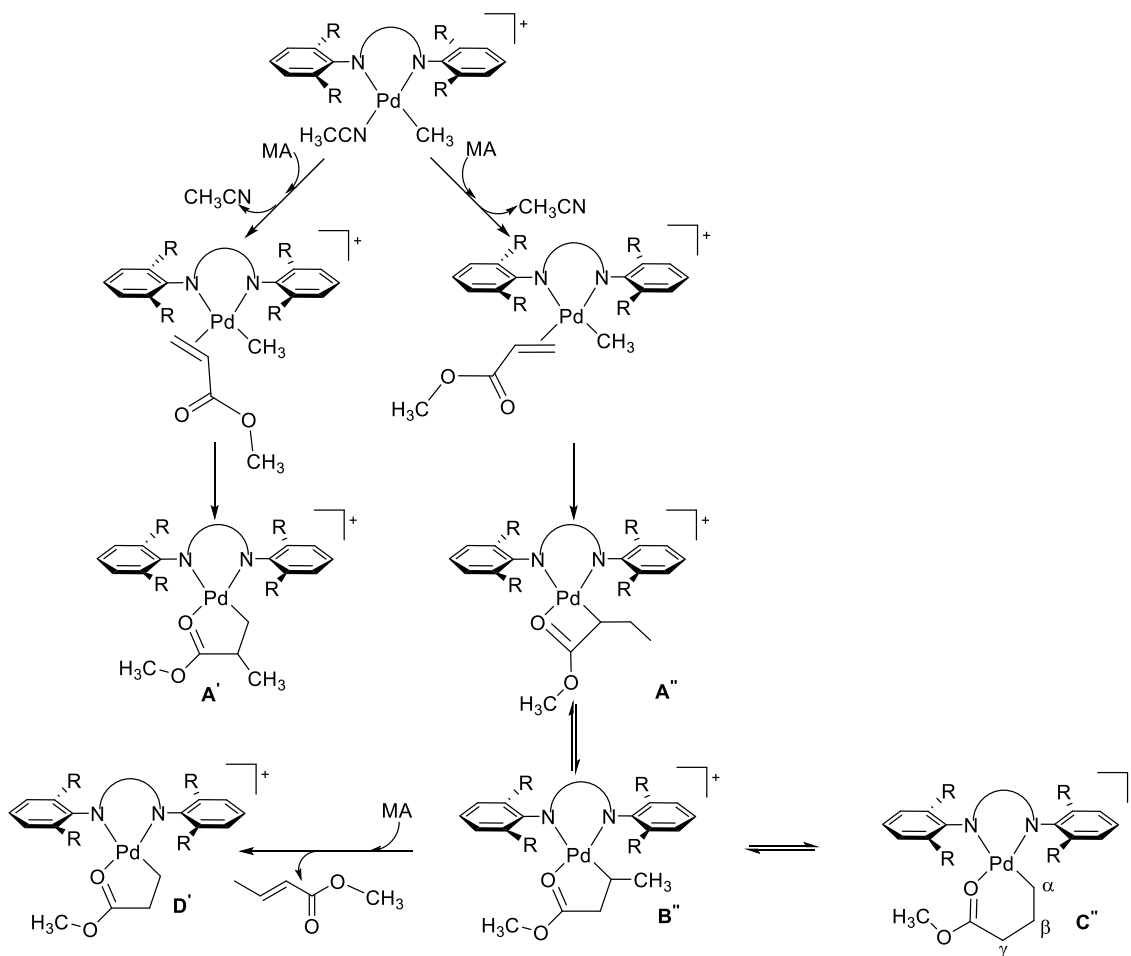
The mechanism of the ethylene/MA copolymerization reaction catalysed by α -diimines-Pd(II) complexes is well established and based on three migratory insertion reactions: that of ethylene either after the insertion of ethylene itself or of methyl acrylate, and that of the polar monomer after the insertion of ethylene.^{2b} It is known from literature that on the Pd-(α -diimine) catalysts the migratory insertion of ethylene is very fast. In the present catalytic system the reactivity of **1b** with ethylene was investigated by bubbling the gaseous monomer into a 10 mM solution of the complex in CD_2Cl_2 at 298 K. In the ^1H NMR spectrum recorded after 6 min from the bubbling, the formation of polyethylene is evident, together with the almost complete

consumption of ethylene and traces of the remaining palladium precursor (Figure S58), thus confirming also for the Pd-(Ar-BIP) complexes the typical reactivity of the Pd-(α -diimine) systems.^{2b, 16a}

The reactivity towards methyl acrylate was studied by adding 2 eq of the polar monomer to a 10 mM solution of **1b**, **2b** and **3b** in CD₂Cl₂, at 298 K. The three precatalysts show a remarkable different reaction rate: for complex **3b** all the precatalyst is consumed after 3 h, whereas for **1b** and **2b** at the same reaction time the 29 and 86 % has reacted, respectively (Figures S59 – S61). Unlike to what is reported for other Pd-(α -diimine) complexes,^{16a} the reaction of **2b** follows a second order kinetic (Figure S62b), whereas for **1b** and **3b** a proper kinetic profile is difficult to model (Figure S62a, S62c).

The established mechanism for the reaction of the Pd-(α -diimine) precatalysts with MA is based on the migratory insertion of the polar monomer into the Pd-CH₃ taking place with either a primary or a secondary regiochemistry, the latter being favoured and followed by the chain walking process that leads to the intermediate C", the catalyst resting state (Scheme 3).^{2b, 16a} The occurring pathway is recognized by the ¹H NMR signals of the typical intermediates. The analysis of the ¹H NMR spectra related to the reactivity of **1b**, **2b** and **3b** with MA points out some differences both among the three complexes and between them and the behaviour of Pd-(Ar-BIAN) and Pd-(Ar-DAB) precatalysts.

Scheme 3. Accepted mechanism for the reaction of Pd-(α -diimine) complexes with MA.



In particular, in the ¹H NMR spectrum of the reaction of **3b** recorded after 1 min from the addition of MA the signals of **3b**, the 5-membered metallacycle **B''** and **C''** are present. The evolution with time indicates that these species are progressively consumed leading to the formation of methyl crotonate, **D'** and **A'**, which are already observed after 15 min of reaction and become the main species after 3 h. These data indicate that β -H elimination is fast and that the insertion of MA into the Pd-CH₃ bond is not highly regioselective (Figure S61).

As far as the reactivity of **2b** is concerned, the signals of the metallacycles **B''**, **C''** and **A'** are observed after 5 min together with those of **2b**. These intermediates are the main species,

together with methyl crotonate and traces of **2b**, at 3 h time. These data indicate that β -H elimination is slower than for **3b** and confirm that the insertion of MA into the Pd-CH₃ bond is not highly regioselective (Figure S60). Therefore, unlike the Pd-(Ar-BIAN) and Pd-(Ar-DAB) precatalysts,^{2b, 16a} for **3b** and **2b** the migratory insertion reaction of MA into the Pd-CH₃ bond is not regiospecific.

Finally, in agreement with the slow reaction rate, in the spectra of **1b** the signals of methyl crotonate and **C''** appear only after 3 h. No peaks due to the other metallacycles are observed. These data indicate that on **1b** the migratory insertion reaction of the polar monomer is very slow, and it is regiospecific (Figure S59).

In the spectra of the reactions of **1b** and **2b** in addition to the signals discussed above, new signals for the substituents on the aryl rings are clearly evident after 15 and 5 min, respectively. Their assignments are in agreement with the X ray analysis in solid state of crystals formed upon addition of *n*-hexane to these solutions kept at 277 K for two weeks.

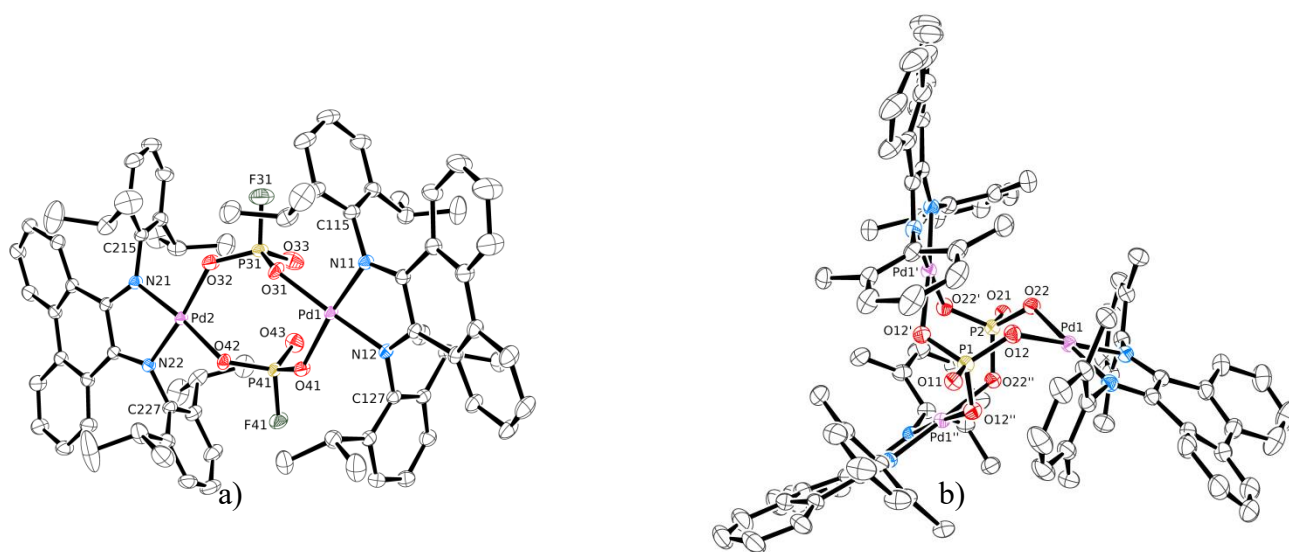


Figure 8. ORTEP drawing (thermal ellipsoids at the 50 % of probability level) for complexes: a) dimer-**1c**; b) trimer-**2c**. Selected bond lengths (Å) for: **1c** Pd(1)-N(11) 1.969(21), Pd(1)-N(12) 1.968(2), Pd(1)-O(31) 2.013(2), Pd(1)-O(41) 2.007(2), Pd(2)-N(21) 1.970(2), Pd(2)-N(22) 1.968(2), Pd(2)-O(32) 2.017(2), Pd(2)-O(42) 2.014(2); **2c** Pd(1)-N 1.976(3), Pd(1)-N 1.973(3), Pd(1)-O(22) 2.024(2), Pd(1)-O(12) 2.021(2).

The crystals obtained from the reaction of **1b** with MA correspond to a dimeric species, **1c**, in which two tetrahedral PO_3F^{2-} ions bridge two Pd atoms (Pd---Pd distance: 5.227(2) Å; Figure 8a). The coordination of each Pd is completed by the Ar-BIP ligand **1**. The crystals obtained from the reaction of **2b** with MA correspond to a trimeric species, **2c**, in which two phosphate groups keep together three Pd moieties, each completed by one Ar-BIP ligand **2** (Figure 8b). Probably due to the increased rigidity of the molecule, the twisting of the Ar-BIP ligand is considerably reduced in **2c** with respect to the corresponding mononuclear complex **2b**, as shown

in Figure 9. The Ar-BIP conformation in **1c** is very similar to that in **2c** (Figure 9): in this case, no crystal structure is available for the corresponding **1b** complex to make a direct comparison.

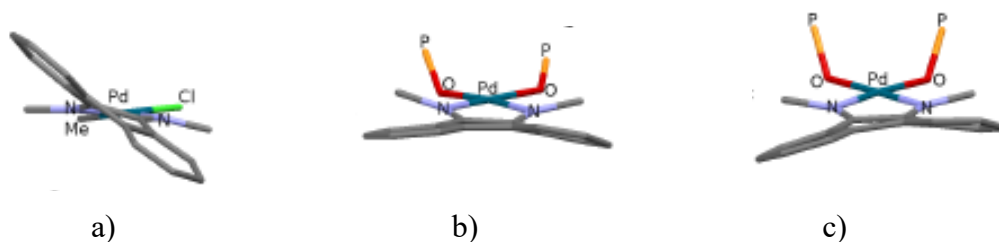


Figure 9. Fragments cut out from the structures of: a) **2b**; b) trimer **2c**; c) dimer **1c**. They put in evidence the decreased twisting of the Ar-BIP ligand on passing from the mononuclear to the multinuclear molecules.

The bridging ions, PO_3F^{2-} and PO_4^{3-} , are probably originated by the partial and full hydrolysis of PF_6^- counterions, respectively. In general, this is not a very common reaction pathway; only a few reports can be found in the literature about metal complexes in which PO_3F^{2-} acts as a bridging ligand and even fewer where this anion connects only two metal centers.³¹ To the best of our knowledge, these are the first structurally characterized examples of Pd complexes of this type.

The combination of the NMR data about the reactivity of complexes **1b**, **2b** and **3b** with MA and the X-ray analysis suggests that the formation of the multinuclear species might represent the deactivation pathway for the Ar-BIP-catalysts and their formation is relevant when the catalytic reaction slows down.

Conclusion

In summary, we have now investigated organometallic palladium(II) complexes with α -diimines having a phenanthrene skeleton and 2,6-disubstituted aryl rings (Ar-BIP). The synthesis of the neutral complexes $[\text{Pd}(\text{Ar-BIP})(\text{CH}_3)\text{Cl}]$ was not as trivial as that typically applied to obtain the same compounds with the corresponding Ar-BIANs. The reasons lie in the lack in solution of the *E,E* isomer, in the remarkable distortion from planarity of the phenanthrene backbone and in the steric hindrance of the substituents in *ortho* positions on the aryl rings. From the neutral derivatives the cationic $[\text{Pd}(\text{Ar-BIP})(\text{CH}_3)(\text{CH}_3\text{CN})][\text{PF}_6]$ compounds were obtained with no difficulties.

The characterization both in solution and in solid state of the two series of complexes points out that Ar-BIP ligands have a higher Lewis basicity than the corresponding Ar-BIAN counterparts and are more strongly bonded to the metal center. In particular, the monocationic derivatives can be regarded as electron-rich metal cations.

The cationic compounds generated efficient catalysts for the ethylene/methyl acrylate copolymerization under mild reaction conditions of temperature and pressure leading to the corresponding copolymers. A detailed investigation of the catalytic behavior was carried out highlighting the main differences with catalysts having the Ar-BIANs. In particular, the Pd-(Ar-BIP) active species show a good affinity towards the polar monomer, a good thermal stability, lead to copolymers of higher molecular weight, and favor the cleavage of the 6-membered metallacycle, recognized as the resting state of the catalytic cycle. All these catalytic findings correlate well with the electron-rich metal cationic feature of the active species.

Detailed NMR characterization of the produced macromolecules probes evidence that the polar vinyl monomer is inserted both at the end of the branches and into the main chain with a more

selective enchainment of that achieved when the copolymerization is carried out in dichloromethane. This aspect is currently under investigation.

This study points out the importance of the ligand skeleton in the design of catalysts for the target reaction and demonstrates that moving from the acenaphthene to the phenanthrene backbone has remarkable influence on both coordination chemistry and catalysis. In addition, it represents the first time that this copolymerization is carried out in a fluorinated solvent highlighting its beneficial effect, in particular on the copolymer microstructure. These results prompt us to investigate the catalytic performances of old and new catalysts in trifluoroethanol.

Currently, we are also focusing on the development of catalysts having the corresponding nonsymmetric Ar,Ar'-BIP to create a subtle steric and electronic unbalance on the two nitrogen-donor atoms that we predict might have a beneficial effect on the catalyst performances.

Supporting Information. The following files are available free of charge.

Experimental section; details on the characterization of the compounds, NMR spectra, X-ray crystallography, tables with catalytic data, GPC traces and NMR spectra of the copolymers, NMR spectra of the in situ reactivity (PDF)
CIF file of solid state structure (CIF)

AUTHOR INFORMATION

Corresponding Author

*E-mail: milaniba@units.it.

ORCID

Barbara Milani: 0000-0002-4466-7566

Gabriele Balducci: 0000-0002-0007-0880

Luca Cusin: 0000-0002-7845-0947

Anna Dall’Anese: 0000-0001-6286-489X

Ilaria D’Auria: 0000-0002-3561-012X

Fulvia Felluga: 0000-0001-8271-408X

Paolo Fornasiero: 0000-0003-1082-9157

Tiziano Montini: 0000-0001-9515-566X

Claudio Pellecchia: 0000-0003-4358-1776

Present Addresses

§ For V.R.: Morgartenstrasse 11, 3014 Bern, Switzerland

§ For L.C.: Università di Bologna, Dipartimento di chimica "Giacomo Ciamician", via Selmi 2,
Bologna, Italy

Author Contributions

The manuscript was written through contributions of all authors. All authors have given approval to the final version of the manuscript.

Funding Sources

MIUR (PRIN 2015, N° 20154X9ATP_005)

Università degli Studi di Trieste, Finanziamento di Ateneo per progetti di ricerca scientifica;
FRA 2018

Notes

The authors declare no competing financial interest.

ACKNOWLEDGMENT. This work was financially supported by MIUR (PRIN 2015, N° 20154X9ATP_005), Università degli Studi di Trieste (Finanziamento di Ateneo per progetti di ricerca scientifica; FRA 2018), INSTM Consortium and ICCOM-CNR. Fondazione Beneficentia Stiftung is gratefully acknowledged for cofinancing the fellowship to A.DA.. Fondazione CRTrieste is gratefully acknowledged for the generous donation of a Varian 500 MHz spectrometer. BASF Italia is acknowledged for a generous donation of [Pd(OAc)₂]. Dr. Nicola Demitri and the staff of the Elettra Synchrotron in Trieste are gratefully acknowledged for assistance in collecting X ray data.

REFERENCES

1. (a) Chen, Z.; Brookhart, M., Exploring Ethylene/Polar Vinyl Monomer Copolymerizations Using Ni and Pd α -Diimine Catalysts. *Acc. Chem. Res.* **2018**, *51* (8), 1831-1839; (b) Guo, L.; Liu, W.; Chen, C., Late transition metal catalyzed α -olefin polymerization and copolymerization with polar monomers. *Mater. Chem. Front.* **2017**, *1* (12), 2487-2494; (c) Guo, L.; Dai, S.; Sui, X.; Chen, C., Palladium and Nickel Catalyzed Chain Walking Olefin Polymerization and Copolymerization. *ACS Catal.* **2016**, *6* (1), 428-441; (d) Chen, Y.; Wang, L.; Yu, H.; Zhao, Y.; Sun, R.; Jing, G.; Huang, J.; Khalid, H.; Abbasi, N. M.; Akram, M., Synthesis and application of polyethylene-based functionalized hyperbranched polymers. *Prog. Polym. Sci.* **2015**, *45*, 23-43; (e) Carrow, B. P.; Nozaki, K., Transition-Metal-Catalyzed Functional Polyolefin Synthesis: Effecting Control through Chelating Ancillary Ligand Design and Mechanistic Insights. *Macromolecules* **2014**, *47* (8), 2541-2555; (f) Rünzi, T.; Mecking, S., Saturated Polar-Substituted Polyethylene Elastomers from Insertion Polymerization. *Adv. Funct. Mat.* **2014**, *24*, 387-395; (g) Nakamura, A.; Anselment, T. M. J.; Claverie, J.; Goodall, B.; Jordan, R. F.; Mecking, S.; Rieger, B.; Sen, A.; Van Leeuwen, P.; Nozaki, K., Ortho-Phosphinobenzenesulfonate: A Superb Ligand for Palladium-Catalyzed Coordination-Insertion Copolymerization of Polar Vinyl Monomers. *Acc. Chem. Res.* **2013**, *46* (7), 1438-1449; (h) Ito, S.; Nozaki, K., Coordination-Insertion Copolymerization of Polar Vinyl Monomers by Palladium Catalysts. *Chem. Rec.* **2010**, *10* (5), 315-325; (i) Nakamura, A.; Ito, S.; Nozaki, K., Coordination-Insertion Copolymerization of Fundamental Polar Monomers. *Chem. Rev.* **2009**, *109* (11), 5215-5244; (j) Boffa, L. S.; Novak, B. M., Copolymerization of Polar Monomers with Olefins Using Transition-Metal Complexes. *Chem. Rev.* **2000**, *100* (4), 1479-1494; (k) Ittel, S. D.; Johnson, L. K.; Brookhart, M., Late-Metal Catalysts for Ethylene Homo- and Copolymerization. *Chem. Rev.* **2000**, *100* (4), 1169-1204; (l) Chen, C., Designing catalysts for olefin polymerization and copolymerization: beyond electronic and steric tuning. *Natrevchem* **2018**, *2*, 6-14; (m) Wang, F.; Chen, C., A continuing legend: the Brookhart-type α -diimine nickel and palladium catalysts. *Polym. Chem.* **2019**, *10* (19), 2354-2369.
2. (a) Johnson, L. K.; Mecking, S.; Brookhart, M., Copolymerization of ethylene and propylene with functionalized vinyl monomers by palladium(II) catalysts. *J. Am. Chem. Soc.* **1996**, *118* (1), 267-268; (b) Mecking, S.; Johnson, L. K.; Wang, L.; Brookhart, M., Mechanistic studies of the palladium-catalyzed copolymerization of ethylene and alpha-olefins with methyl acrylate. *J. Am. Chem. Soc.* **1998**, *120* (5), 888-899.
3. Drent, E.; van Dijk, R.; van Ginkel, R.; van Oort, B.; Pugh, R. I., Palladium catalysed copolymerisation of ethene with alkylacrylates: polar comonomer built into the linear polymer chain. *Chem. Commun.* **2002**, (7), 744-745.
4. (a) Mitsushige, Y.; Yasuda, H.; Carrow, B. P.; Ito, S.; Kobayashi, M.; Tayano, T.; Watanabe, Y.; Okuno, Y.; Hayashi, S.; Kuroda, J.; Okumura, Y.; Nozaki, K., Methylene-Bridged Bisphosphine Monoxide Ligands for Palladium-Catalyzed Copolymerization of Ethylene and Polar Monomers. *ACS Macro Lett.* **2018**, *7* (3), 305-311; (b) Mitsushige, Y.; Carrow, B. P.; Ito, S.; Nozaki, K., Ligand-controlled insertion regioselectivity accelerates copolymerisation of ethylene with methyl acrylate by cationic bisphosphine monoxide-palladium catalysts. *Chem.Sci.* **2016**, *7* (1), 737-744; (c) Carrow, B. P.; Nozaki, K., Synthesis of Functional Polyolefins Using Cationic Bisphosphine Monoxide-Palladium Complexes. *J. Am. Chem. Soc.* **2012**, *134* (21), 8802-8805.

5. (a) Nakano, R.; Nozaki, K., Copolymerization of Propylene and Polar Monomers Using Pd/IzQO Catalysts. *J. Am. Chem. Soc.* **2015**, *137* (34), 10934-10937; (b) Yasuda, H.; Nakano, R.; Ito, S.; Nozaki, K., Palladium/IZQO-Catalyzed coordination-insertion copolymerization of ethylene and 1,1-disubstituted ethylenes bearing a polar functional group. *J. Am. Chem. Soc.* **2018**, *140*, 1876-1883.
6. Tao, W.; Akita, S.; Nakano, R.; Ito, S.; Hoshimoto, Y.; Ogoshi, S.; Nozaki, K., Copolymerisation of ethylene with polar monomers by using palladium catalysts bearing an N-heterocyclic carbene-phosphine oxide bidentate ligand. *Chem. Commun.* **2017**, *53* (17), 2630-2633.
7. Zhang, W.; Waddell, P. M.; Tiedemann, M. A.; Padilla, C. E.; Mei, J.; Chen, L.; Carrow, B. P., Electron-rich metal cations enable synthesis of high molecular weight, linear functional polyethylenes. *J. Am. Chem. Soc.* **2018**, *140*, 8841-8850.
8. Hu, H.; Chen, D.; Gao, H.; Zhong, L.; Wu, Q., Amine-imine palladium catalysts for living polymerization of ethylene and copolymerization of ethylene with methyl acrylate: incorporation of acrylate units into the main chain and branch end. *Polym. Chem.* **2016**, *7* (3), 529-537.
9. Heyndrickx, W.; Occhipinti, G.; Bultinck, P.; Jensen, V. R., Striking a Compromise: Polar Functional Group Tolerance versus Insertion Barrier Height for Olefin Polymerization Catalysts. *Organometallics* **2012**, *31* (17), 6022-6031.
10. (a) Zhong, L.; Li, G.; Liang, G.; Gao, H.; Wu, Q., Enhancing Thermal Stability and Living Fashion in α -Diimine-Nickel-Catalyzed (Co)polymerization of Ethylene and Polar Monomer by Increasing the Steric Bulk of Ligand Backbone. *Macromolecules* **2017**, *50* (7), 2675-2682; (b) Chen, M.; Chen, C., Rational Design of High-Performance Phosphine Sulfonate Nickel Catalysts for Ethylene Polymerization and Copolymerization with Polar Monomers. *ACS Catal.* **2017**, *7* (2), 1308-1312; (c) Xin, B. S.; Sato, N.; Tanna, A.; Oishi, Y.; Konishi, Y.; Shimizu, F., Nickel Catalyzed Copolymerization of Ethylene and Alkyl Acrylates. *J. Am. Chem. Soc.* **2017**, *139* (10), 3611-3614; (d) Zhang, Y.; Mu, H.; Pan, L.; Wang, X.; Li, Y., Robust Bulky [P,O] Neutral Nickel Catalysts for Copolymerization of Ethylene with Polar Vinyl Monomers. *ACS Catal.* **2018**, *8* (7), 5963-5976; (e) Xia, J.; Zhang, Y.; Zhang, J.; Jian, Z., High-Performance Neutral Phosphine-Sulfonate Nickel(II) Catalysts for Efficient Ethylene Polymerization and Copolymerization with Polar Monomers. *Organometallics* **2019**, *38* (5), 1118-1126; (f) Kanai, Y.; Foro, S.; Plenio, H., Bispentipycenyl-Diimine-Nickel Complexes for Ethene Polymerization and Copolymerization with Polar Monomers. *Organometallics* **2019**, *38* (2), 544-551.
11. (a) Popeney, C. S.; Camacho, D. H.; Guan, Z., Efficient Incorporation of Polar Comonomers in Copolymerizations with Ethylene Using a Cyclophane-Based Pd(II) α -Diimine Catalyst. *J. Am. Chem. Soc.* **2007**, *129*, 10062-10063; (b) Popeney, C. S.; Guan, Z., A Mechanistic Investigation on Copolymerization of Ethylene with Polar Monomers Using a Cyclophane-Based Pd(II) α -Diimine Catalyst. *J. Am. Chem. Soc.* **2009**, *131* (34), 12384-12393.
12. Takano, S.; Takeuchi, D.; Osakada, K.; Akamatsu, N.; Shishido, A., Dipalladium Catalyst for Olefin Polymerization: Introduction of Acrylate Units into the Main Chain of Branched Polyethylene. *Angew. Chem. Int. Ed.* **2014**, *53* (35), 9246-9250.
13. (a) Dai, S.; Sui, X.; Chen, C., Highly Robust Palladium(II) α -Diimine Catalysts for Slow-Chain-Walking Polymerization of Ethylene and Copolymerization with Methyl Acrylate. *Angew. Chem. Int. Ed.* **2015**, *54* (34), 9948-9953; (b) Ma, X.; Hu, X.; Zhang, Y.; Mu, H.; Cui, L.; Jian,

- Z., Preparation and in situ chain-end-functionalization of branched ethylene oligomers by monosubstituted α -diimine nickel catalysts. *Polym. Chem.* **2019**, *10* (20), 2596-2607.
14. Liao, Y.; Zhang, Y.; Cui, L.; Mu, H.; Jian, Z., Pentiptycenyyl Substituents in Insertion Polymerization with α -Diimine Nickel and Palladium Species. *Organometallics* **2019**, *38* (9), 2075-2083.
15. Allen, K. E.; Campos, J.; Daugulis, O.; Brookhart, M., Living Polymerization of Ethylene and Copolymerization of Ethylene/Methyl Acrylate Using "Sandwich" Diimine Palladium Catalysts. *ACS Catal.* **2015**, *5* (1), 456-464.
16. (a) Meduri, A.; Montini, T.; Ragaini, F.; Fornasiero, P.; Zangrando, E.; Milani, B., Palladium-Catalyzed Ethylene/Methyl Acrylate Cooligomerization: Effect of a New Nonsymmetric α -Diimine. *ChemCatChem* **2013**, *5* (5), 1170-1183; (b) Rosar, V.; Montini, T.; Balducci, G.; Zangrando, E.; Fornasiero, P.; Milani, B., Palladium-Catalyzed Ethylene/Methyl Acrylate Co-Oligomerization: The Effect of a New Nonsymmetrical α -Diimine with the 1,4-Diazabutadiene Skeleton. *ChemCatChem* **2017**, *9* (17), 3402-3411; (c) Rosar, V.; Meduri, A.; Montini, T.; Fornasiero, P.; Zangrando, E.; Milani, B., The contradictory effect of the methoxy-substituent in palladium-catalyzed ethylene/methyl acrylate cooligomerization. *Dalton Trans.* **2018**, *47* (8), 2778-2790.
17. Guo, L.; Gao, H.; Guan, Q.; Hu, H.; Deng, J.; Liu, J.; Liu, F.; Wu, Q., Substituent Effects of the Backbone in $\hat{\pm}$ -Diimine Palladium Catalysts on Homo- and Copolymerization of Ethylene with Methyl Acrylate. *Organometallics* **2012**, *31* (17), 6054-6062.
18. Zou, W.; Chen, C., Influence of Backbone Substituents on the Ethylene (Co)polymerization Properties of α -diimine Pd(II) and Ni(II) Catalysts. *Organometallics* **2016**, *35* (11), 1794-1801.
19. Zhong, S.; Tan, Y.; Zhong, L.; Gao, J.; Liao, H.; Jiang, L.; Gao, H.; Wu, Q., Precision Synthesis of Ethylene and Polar Monomer Copolymers by Palladium-Catalyzed Living Coordination Copolymerization. *Macromolecules* **2017**, *50* (15), 5661-5669.
20. van Belzen, R.; Klein, R. A.; Smeets, W. J. J.; Spek, A. L.; Benedix, R.; Elsevier, C. J., Synthesis and characterization of 9,10-bis(arylimino)-9,10-dihydrophenanthrenes, the structure of (Z,Z)-9,10-bis(phenylimino)-9,10-dihydrophenanthrene and PdCl₂-[(E,E)-9,10-bis(phenylimino)-9,10-dihydrophenanthrene] in the solid state and in solution. *Rec.Trav. Chim. Pays-Bas* **1996**, *115*, 275-285.
21. (a) Gao, B.; Zhao, D.; Li, X.; Cui, Y.; Duan, R.; Pang, X., Magnesium complexes bearing N,N-bidentate phenanthrene derivatives for the stereoselective ring-opening polymerization of rac-lactides. *RSC Adv.* **2015**, *5* (1), 440-447; (b) Li, L.; Jeon, M.; Kim, S. Y., Synthesis, characterization and ethylene polymerisation of 9,10-phenanthrenequinone-based nickel(II)- α -diimine complexes. *J. Mol. Cat. A: Chemical* **2009**, *303* (1), 110-116; (c) Gao, B.; Luo, X.; Gao, W.; Huang, L.; Gao, S.-m.; Liu, X.; Wu, Q.; Mu, Y., Chromium complexes supported by phenanthrene-imine derivative ligands: synthesis, characterization and catalysis on isoprenecis-1,4 polymerization. *Dalton Trans.* **2012**, *41* (9), 2755-2763.
22. Cherkasov, V. K.; Druzhkov, N. O.; Kocherova, T. N.; Shavyrin, A. S.; Fukin, G. K., N,N'-Disubstituted phenanthrene-9,10-diimines: synthesis and NMR spectroscopic study. *Tetrahedron* **2012**, *68* (5), 1422-1426.
23. (a) Hill, N. J.; Vargás-Baca, I.; Cowley, A. H., Recent developments in the coordination chemistry of bis(imino)acenaphthene (BIAN) ligands with s- and p-block elements. *Dalton Trans.* **2009**, (2), 240-253; (b) Rosar, V.; Meduri, A.; Montini, T.; Fini, F.; Carfagna, C.; Fornasiero, P.; Balducci, G.; Zangrando, E.; Milani, B., Analogies and Differences in Palladium-

Catalyzed CO/Styrene and Ethylene/Methyl Acrylate Copolymerization Reactions.

ChemCatChem **2014**, *6* (8), 2403-2418; (c) van Asselt, R.; Elsevier, C. J.; Smeets, W. J. J.; Spek, A. L.; Benedix, R., Synthesis and characterization of rigid bidentate nitrogen ligands and some examples of coordination to divalent palladium. X-ray crystal structures of bis (p-tolylimino) acenaphthene and methylchloro [bis(o,o'-diisopropylphenyl-imino) acenaphthene] palladium (II). *Rec. Trav. Chim. Pays-Bas* **1994**, *113* (2), 88-98.

24. (a) Rülke, R. E.; Ernsting, J. M.; Spek, A. L.; Elsevier, C. J.; Van Leeuwen, P. W. N. M.; Vrieze, K., NMR Study on the Coordination Behavior of Dissymmetric Terdentate Trinitrogen Ligands on Methylpalladium(II) Compounds. *Inorg. Chem.* **1993**, *32*, 5769-5778; (b) Durand, J.; Zangrando, E.; Stener, M.; Fronzoni, G.; Carfagna, C.; Binotti, B.; Kamer, P. C. J.; Muller, C.; Caporali, M.; van Leeuwen, P. W. N. M.; Vogt, D.; Milani, B., Long-Lived Palladium Catalysts for CO/Vinyl Arene Polyketones Synthesis: A Solution to Deactivation Problems. *Chem. Eur. J.* **2006**, *12*, 7639-7651.

25. Khlebnikov, V.; Meduri, A.; Mueller-Bunz, H.; Montini, T.; Fornasiero, P.; Zangrando, E.; Milani, B.; Albrecht, M., Palladium Carbene Complexes for Selective Alkene Di- and Oligomerization. *Organometallics* **2012**, *31* (3), 976-986.

26. Rosar, V.; Dedeic, D.; Nobile, T.; Fini, F.; Balducci, G.; Alessio, E.; Carfagna, C.; Milani, B., Palladium complexes with simple iminopyridines as catalysts for polyketone synthesis. *Dalton Trans.* **2016**, *45* (37), 14609-14619.

27. Johnson, L. K.; Killian, C. M.; Brookhart, M., New Pd(II)-Based and Ni(II)-Based Catalysts for Polymerization of Ethylene and Alpha-Olefins. *J. Am. Chem. Soc.* **1995**, *117* (23), 6414-6415.

28. Szabo, M. J.; Jordan, R. F.; Michalak, A.; Piers, W. E.; Weiss, T.; Yang, S.-Y.; Ziegler, T., Polar Copolymerization by a Palladium–Diimine-Based Catalyst. Influence of the Catalyst Charge and Polar Substituent on Catalyst Poisoning and Polymerization Activity. A Density Functional Theory Study. *Organometallics* **2004**, *23* (23), 5565-5572.

29. (a) Berkefeld, A.; Drexler, M.; Moller, H. M.; Mecking, S., Mechanistic Insights on the Copolymerization of Polar Vinyl Monomers with Neutral Ni(II) Catalysts. *J. Am. Chem. Soc.* **2009**, *131* (35), 12613-12622; (b) Usami, T.; Takayama, S., Fine-branching structure in high-pressure, low-density polyethylenes by 50.10-MHz carbon-13 NMR analysis. *Macromolecules* **1984**, *17* (9), 1756-1761; (c) Axelson, D. E.; Levy, G. C.; Mandelkern, L., A Quantitative Analysis of Low-Density (Branched) Polyethylenes by Carbon-13 Fourier Transform Nuclear Magnetic Resonance at 67.9 MHz. *Macromolecules* **1979**, *12* (1), 41-52; (d) McCord, E. F.; McLain, S. J.; Nelson, L. T. J.; Arthur, S. D.; Coughlin, E. B.; Ittel, S. D.; Johnson, L. K.; Tempel, D.; Killian, C. M.; Brookhart, M., ¹³C and 2D NMR Analysis of Propylene Polymers Made with α -Diimine Late Metal Catalysts. *Macromolecules* **2001**, *34* (3), 362-371; (e) McCord, E. F.; McLain, S. J.; Nelson, L. T. J.; Ittel, S. D.; Tempel, D.; Killian, C. M.; Johnson, L. K.; Brookhart, M., ¹³C NMR Analysis of $\hat{I}\pm$ -Olefin Enchainment in Poly($\hat{I}\pm$ -olefins) Produced with Nickel and Palladium $\hat{I}\pm$ -Diimine Catalysts. *Macromolecules* **2007**, *40* (3), 410-420.

30. Contrella, N. D.; Sampson, J. R.; Jordan, R. F., Copolymerization of Ethylene and Methyl Acrylate by Cationic Palladium Catalysts That Contain Phosphine-Diethyl Phosphonate Ancillary Ligands. *Organometallics* **2014**, *33* (13), 3546-3555.

31. (a) Dermitzaki, D.; Raptopoulou, C. P.; Psycharis, V.; Escuer, A.; Perlepes, S. P.; Stamatatos, T. C., Unexpected metal ion-assisted transformations leading to unexplored bridging ligands in Ni(II) coordination chemistry: the case of PO₃F₂⁻ group. *Dalton Trans.* **2014**, *43* (39), 14520-14524; (b) Konidaris, K. F.; Polyzou, C. D.; Kostakis, G. E.; Tasiopoulos, A. J.; Roubeau,

O.; Teat, S. J.; Manessi-Zoupa, E.; Powell, A. K.; Perlepes, S. P., Metal ion-assisted transformations of 2-pyridinealdoxime and hexafluorophosphate. *Dalton Trans.* **2012**, 41 (10), 2862-2865; (c) Fernandez-Galan, R.; Manzano, B. R.; Otero, A.; Lanfranchi, M.; Pellinghelli, M. A., ^{19}F and ^{31}P NMR evidence for silver hexafluorophosphate hydrolysis in solution. New palladium difluorophosphate complexes and X-ray structure determination of $[\text{Pd}(\eta^3\text{-2-Me-C}_3\text{H}_4)(\text{PO}_2\text{F}_2)(\text{PCy}_3)]$. *Inorg. Chem.* **1994**, 33, 2309-2312.

For Table of Contents only

